

# Analysis of Human Fibroadenomas using Three-dimensional Impedance Maps

Alexander Dapore<sup>1</sup>, Michael R. King<sup>1</sup>, Josephine Harter<sup>2</sup>, Sandhya Sarwate<sup>1</sup>,  
Michael L. Oelze<sup>1</sup>, James A. Zagzebski<sup>2</sup>, Minh N. Do<sup>1</sup>, Timothy J. Hall<sup>2</sup>, William D. O'Brien, Jr.<sup>1</sup>

<sup>1</sup>Bioacoustics Research Laboratory, Department of Electrical and Computer Engineering  
University of Illinois at Urbana-Champaign, Urbana, IL, 61801

<sup>2</sup> Department of Medical Physics, University of Wisconsin-Madison, Madison, WI, 53706  
Email: adapore2@illinois.edu

**Abstract**—Three-dimensional impedance maps (3DZMs) are virtual volumes of acoustic impedance values constructed from histology to represent tissue microstructure acoustically. From the 3DZM, estimations can be made for ultrasonic backscatter and scatterer properties, such as effective scatterer diameter (ESD). Additionally, the 3DZM can be exploited to visualize and identify possible scattering sites, which may aid in the development of more effective scattering models to better represent the ultrasonic interaction with underlying tissue microstructure.

In this study, 3DZMs were created from several human fibroadenoma samples. ESD estimates were obtained using the fluid-filled sphere form factor model. These estimates were made using two regions of interest (ROIs) sizes: cubes of side length 300  $\mu\text{m}$  and 150  $\mu\text{m}$ . This estimation technique allowed a better understanding of the spatial distribution and variability of the estimates throughout the volume. For a collection of 33 3DZMs, the ESD was estimated to be  $99 \pm 43 \mu\text{m}$  with the large ROI and  $65 \pm 30 \mu\text{m}$  when using the small ROI. The 3DZMs were then investigated visually to identify possible scattering sources, which conformed to the estimated characteristic scatterer dimensions. This visualization and comparison resulted in the identification of possible ultrasonic scattering sources within human fibroadenomas.

## I. INTRODUCTION

Medical ultrasound provides both a safe and an inexpensive imaging modality when compared to other common modalities such as X-ray, computed tomography, or magnetic resonance imaging [1], [2]. These advantages clearly motivate the development of additional diagnostic functionality in medical ultrasound. While conventional ultrasound images provide only qualitative depictions of tissue macrostructure, quantitative ultrasound (QUS) seeks to provide quantitative information about tissue on a smaller scale. This information could greatly improve the diagnostic functionality in medical ultrasound. However, this process depends on the use of appropriate models for ultrasonic scattering by tissue microstructure [3].

As a means to investigate such ultrasonic scattering, a method was previously developed to create computational acoustic models of tissue microstructure [1]. These models, called three-dimensional impedance maps (3DZMs), provide a means to combine ultrasonic characterization of tissue with histological evaluation of the underlying tissue structure. This study investigates the application of these models to a common type of benign human breast tumor, the fibroadenoma. These

results were then compared to the histological features of the tissue to help identify possible scattering sources.

### A. Quantitative Ultrasound

Conventional ultrasound images are derived from backscattered radio frequency (RF) echo signals, which are a result of scattering by tissue macro- and microstructure with varying acoustic properties. Typically, the received RF signals are envelope-detected to produce an image, but this processing removes frequency-dependent information from the RF signal [4].

QUS uses the frequency dependent information from the RF echo signal to deduce quantitative information related to the properties of the tissue microstructure. This frequency dependent information can provide details about statistical properties of scattering structures, such as effective scatterer size (ESD) and effective scatterer concentration. Parameterization of ultrasonic backscatter has been investigated previously as a means to extend the diagnostic capability of ultrasound [5], [6], and has demonstrated the ability to quantify ocular, liver, prostate, renal, and cardiac tissues [7]. To attain more meaningful results, however, the relationship between backscattered frequency dependent information and underlying tissue properties must be better understood.

### B. Three-Dimensional Impedance Maps

A 3DZM is an acoustic, computational model of tissue, and a tool to aid in the understanding of small scale acoustic scattering. Currently, 3DZMs are volumes constructed from properly aligned and reconstructed sets of histological images. The value of each volume element (voxel) of the 3DZM represents an acoustic impedance value.

For media in which the variations in impedance are relatively small, this spatial impedance function can be related to the ultrasonic backscatter of the media by the spatial Fourier transform. In this way, 3DZMs can be used to study both the ultrasonic backscatter and the histological characteristics of a particular medium. This duality illustrates the utility of 3DZMs for the study of ultrasonic scattering in tissue as it relates ultrasonic backscatter to actual histological features of tissue microstructure.

## II. THEORY

### A. Quantitative Ultrasound

Ultrasonic scattering occurs when an incident pressure wave interacts with a volume with spatially varying acoustic properties. Ultrasonic backscatter is defined as the portion of this scattered sound that propagates in the opposite direction of the incident wave, which is of special interest for pulse-echo ultrasound [2]. Under the assumption of weak scattering (acoustic properties of scattering sites are close to those of the surrounding medium) backscattered intensity can be calculated as a function of frequency [1], [6]. Given an acoustic impedance  $z_s$  of the scattering body and a background acoustic impedance  $z_0$ , the backscattered intensity is given by the volume integral

$$S(2k) = \left| \iiint_V \frac{z(r) - z_0}{z_0} e^{-2jkr} dV \right|^2 \quad (1)$$

where  $z(r)$  is the acoustic impedance as a function of position and the acoustic wave number  $k$  is defined as the ratio of the angular frequency of the acoustic wave to the speed of sound in the medium. Equation (1) is equivalent to the squared modulus of the spatial Fourier transform, or the power spectrum, of the relative impedance function [8].

1) *Intensity Form Factor*: Intensity form factors (FFs) are functions which describe the behavior of the backscattered intensity due to a single scattering volume as a function of  $k$  [9]. Form factors model the deviation in the frequency dependence of the backscatter coefficient for a particular scattering volume from the frequency dependence observed for a Rayleigh scatterer (which has only a  $k^4$  dependence). Regardless of the scattering volume geometry, the corresponding FF always approaches unity as  $k$  approaches zero because as the wavelength becomes very large, the scatterer appears as a point scatterer.

Form factors are related to the geometry of the scattering volume by the Fourier transform of the 3D spatial auto-correlation function of the volume, or equivalently by the squared magnitude of the 3D spatial Fourier transform of the volume (due to the Wiener-Khinchine theorem) [8]. Because of this, FFs are proportional to the power spectrum  $S(2k)$  of a scattering volume as described by Equation (1).

The FF model used in this work is the fluid-filled sphere. This FF describes the acoustic scattering from a filled spherical volume of radius  $a$  and acoustic impedance  $z_s$  in a background of impedance  $z_0$ . This FF is expressed as

$$F_a(2k) = \left( \frac{3j_1(2ka)}{2ka} \right)^2 \quad (2)$$

where  $j_1$  is the spherical Bessel function of the first kind. The FF is observed to be a function of  $k$  which depends only on the parameter  $a$ , the sphere radius. Equation (2) is also known to be the 3D Fourier transform of a sphere [6]. For a constant speed of sound, Figure 1 shows a plot of the fluid-filled sphere FF as a function of frequency for several values of  $a$ .

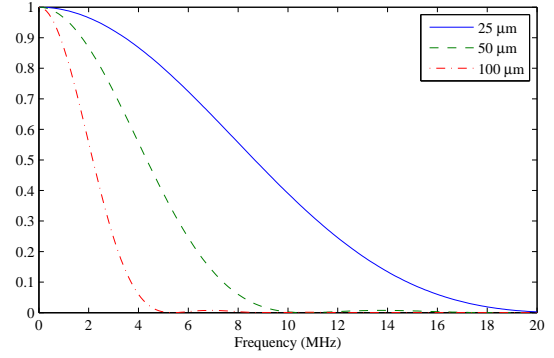


Fig. 1. Fluid-filled form factor for  $a = 25, 50, 100\mu\text{m}$

## III. ACOUSTIC MODELING OF TISSUE

### A. 3DZM Construction

A 3DZM is a computational phantom of which each element represents an estimate of the acoustic impedance value of the underlying medium. A technique for the creation of 3DZMs was developed previously by Mamou [1]. In the current study, a novel 3DZM construction process has been developed that improves upon the method of Mamou has been improved in terms of both performance and computational efficiency.

The 3DZM creation process begins with a tissue sample that has been fixed in formalin, embedded in paraffin, sectioned at a thickness of  $3\mu\text{m}$ , placed on glass slides, and stained with hematoxylin and eosin (H&E). These slides are digitized using NanoZoomer HT slide scanner (Hamamatsu, Hamamatsu City, Japan) at a pixel resolution of  $0.46\mu\text{m}$ . The image is quantized in red, green, and blue color fields (RGB color), at 24 bits per pixel. In order for this set of 2D images be converted into a 3D volume, artifacts inherent to the preparation process must be corrected.

First, the images need to be properly registered to each adjacent section so that the position within the original volume is properly restored. In addition to simple translational and rotational (rigid) registration, the sections must be adjusted for any stretching or shearing that occurred as a result of the tissue slicing. Registration parameters are optimized using a mutual information metric in order to improve robustness [1]. The implementation of the registration algorithm takes advantage of a multiresolution optimization scheme, which greatly reduces computation time in addition to improving the registration quality [10].

Second, the photometric properties of the tissue must be equalized. Slight variation in the thickness of each section results in varying uptake of the H&E stain. This artifact of the slide preparation process is corrected by matching the first order color statistics of each image in the set to a reference image, which is typically the first image of the set. Both mean and variance of each individual color field (RGB) are scaled to match the reference image.

Following the registration and photometric adjustment steps, the computed transformations are applied to each image and

Color	Tissue Component	Impedance Value Range (Mrayls)
Light to Dark Pink	Cytoplasm	1.5 - 1.7
Light to Dark Blue	Cell Nuclei	1.8 - 2.0
White	Fat	1.45

TABLE I  
ACOUSTIC IMPEDANCE ASSIGNMENT SCHEME

a volume is assembled. However, some sections are inadvertently destroyed during the sectioning process, so these missing sections must be filled in to complete the reconstruction of the tissue volume. These missing sections are replaced by interpolated sections by using cubic Hermite interpolation along each stacked column of pixels and independently for each color field [1].

Finally, each element of the tissue volume must be assigned an acoustic impedance value. This is done based on the color value of the pixel, because the H&E staining causes tissue with a greater protein concentration to appear pink and tissue with a greater nucleic acid concentration to appear blue, thus differentiating the underlying tissue components. Impedance values were assigned by associating appropriate acoustic impedance values for each tissue structure with certain color ranges [1]. Tissue areas with eosin staining (indicating protein concentration) range in color from light pink to dark pink, while tissue areas with hematoxylin staining (indicating nucleic acid concentration) range in color from light blue to dark blue. For this work, it was assumed that the pink image elements represented cell cytoplasm, while the blue image elements represented cell nuclei. Other image elements which appeared very light or white were assumed to be fat. Thus, impedance values were assigned based on image color as indicated in Table 1.

### B. Impedance Map Analysis

As a result of the relationship between backscattered intensity and the squared magnitude of the spatial Fourier transform of a medium's relative impedance function, 3DZMs present a useful tool for the study of ultrasonic scattering in tissue. This relationship can be exploited in two ways. First, by assuming some form factor model, an estimate of the effective scatterer size in the 3DZM can be obtained. Second, by using the 3DZM to investigate the layout of the tissue microstructure from an acoustic perspective, new scattering models may be developed which better represent the underlying tissue structure.

1) *Spectral Estimation*: Spectral estimation refers to the signal processing steps taken to compute the power spectrum of a 3DZM. In this step, the underlying tissue is treated as a random and isotropic medium, for which it is desired to estimate the statistical power spectrum using the limited spatial samples of the volume.

The 3D spatial Fourier transform of a volume produces a 3D function of the spatial frequency vector  $\mathbf{k} = k_x\hat{x} + k_y\hat{y} + k_z\hat{z}$ . In the special case of a spherically symmetric scatterer, the Fourier coefficients along each radial path away from  $\mathbf{k} = \vec{0}$

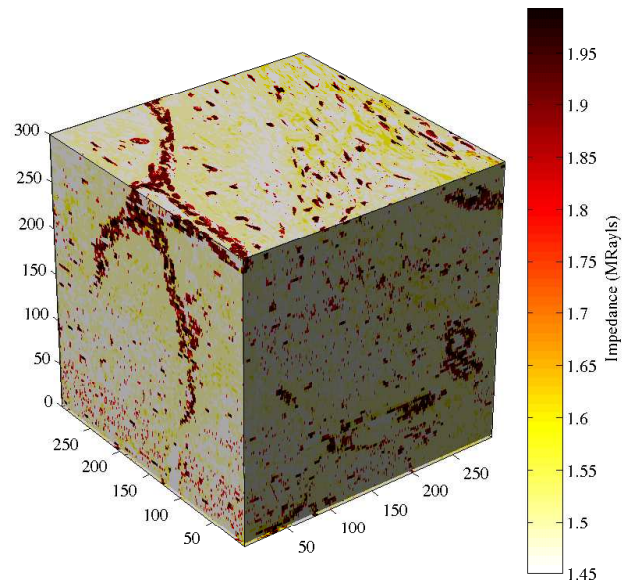


Fig. 2. Rendering of a human fibroadenoma 3DZM

are equal, regardless of which path is chosen; thus, the value of the 3D spatial Fourier transform along any such path is equal to the acoustic form factor of the medium, with the wave number  $k = \sqrt{k_x^2 + k_y^2 + k_z^2}$ . For an  $M$ -by- $N$ -by- $P$  element 3D volume  $f(x, y, z)$ , the 3D spatial discrete Fourier transform in the  $\hat{x}$  direction is given by

$$F(k_x, 0, 0) = \frac{1}{MNP} \sum_{x=0}^{M-1} \left[ \sum_{y=0}^{N-1} \sum_{z=0}^{P-1} f(x, y, z) \right] e^{-j2\pi(k_x x)} \quad (3)$$

The selection of the radial paths for which two of the spatial frequency variables are equal to zero greatly simplifies the computation of this transform. For an ensemble of randomly positioned, identical spherical scatterers, coherent scattering adds random variation to the underlying scattering function [6]. This term is spatially dependent, so different radial paths of the 3D spatial Fourier transform will have different coherent scattering terms. Thus, averaging multiple radial slices of the 3D spatial Fourier transform together serves to reduce the effects of the coherent scattering term. This was done using the three orthogonal radial paths along which  $k = k_x$ ,  $k = k_y$ , and  $k = k_z$  by using an appropriately modified form of Equation (3).

### C. Scatter Size Estimation

Scatterer size estimation is the task of fitting a theoretical FF to the calculated power spectrum of a 3DZM to produce an estimate of the ESD. FFs of spherically symmetric scatterers, like the fluid-filled sphere FF described by Equation (2), have a frequency dependence that scales as a function of scatterer size. Thus, a best-fit curve with respect to mean squared error is used to determine the ESD estimate using a particular theoretical FF.

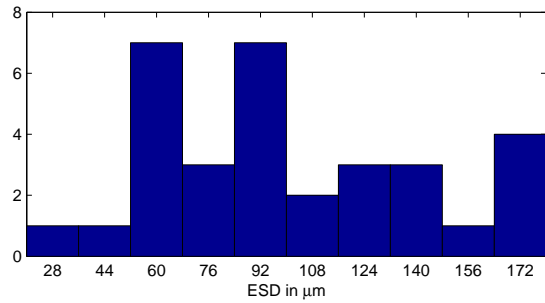


Fig. 3. Histogram of ESD estimates obtained from 33 human fibroadenoma  $300 \times 300 \times 300 \mu\text{m}^3$  ROIs

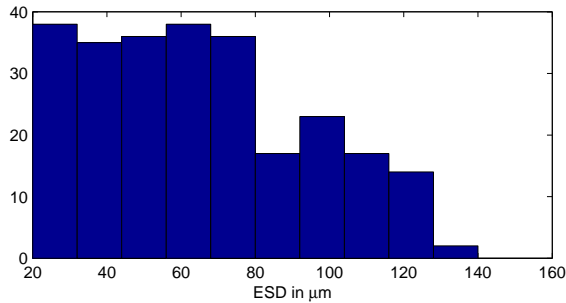


Fig. 4. Histogram of ESD estimates obtained from 264 human fibroadenoma  $150 \times 150 \times 150 \mu\text{m}^3$  ROIs

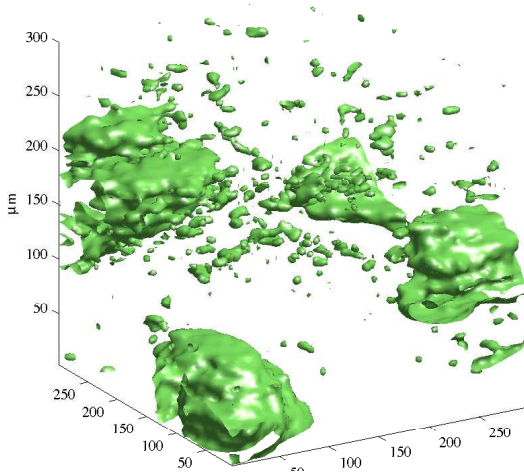


Fig. 5. Surfaces in a 3DZM with impedance values in the range of 1.8 to 2.0 Mrayl. ESD estimates for this 3DZM are  $149 \mu\text{m}$

#### IV. RESULTS

3DZMs were constructed and analyzed for 33 independent human fibroadenoma data sets. For each data set, one  $300 \times 300 \times 300 \mu\text{m}^3$  3DZM was created. Additionally, each 3DZM was split into eight non-overlapping  $150 \mu\text{m}^3$  3DZMs. The scattering model used for analysis was the fluid-filled sphere FF. Figure 3 and figure 4 show histograms of the ESD estimates obtained by using the large and small sized 3DZMs,

respectively.

Figure 5 shows a segmentation of the high and low impedance structures inside one of the human fibroadenoma 3DZMs in this study. Distinct structures of a size corresponding to ESD estimates can be observed inside the volume. The impedance structure of microtissue, observable via the 3DZM method, is potentially a valuable tool in the further development of ultrasonic scattering models.

#### V. CONCLUSION

3DZMs are a unique tool for the study of ultrasonic scattering in tissue. The ability to easily create 3DZMs from histology data was demonstrated, and some analysis techniques and applications of the resulting 3DZMs were explored.

This work focused on the specifics of 3DZM creation and analysis. These techniques were demonstrated on a set of 33 3DZMs created from human fibroadenomas; the results were then used to learn more about possible ultrasonic scattering sources.

Quantitative ultrasound holds great diagnostic potential, and 3DZMs provide a powerful means to relate QUS results to actual tissue microstructure. That is, 3DZMs allow a connection to be made between QUS parameters and tissue pathology. This connection could be an essential step to propel QUS forward as an effective and noninvasive diagnostic imaging modality.

#### ACKNOWLEDGMENT

This work was supported by NIH Grant CA111289.

#### REFERENCES

- [1] J. Mamou, "Ultrasonic characterization of three animal mammary tumors from three-dimensional acoustic tissue models," Ph.D. dissertation, University of Illinois at Urbana-Champaign, Urbana, IL, 2005.
- [2] R. S. C. Cobbold, *Foundations of Biomedical Ultrasound*. New York, NY: Oxford University Press, 1997.
- [3] M. L. Oelze, W. D. O'Brien, Jr., and J. F. Zachary, "Quantitative ultrasound assessment of breast cancer using a multiparameter approach," *Proceedings of the 2007 IEEE Ultrasonics Symposium*, 2007, pp. 981-984.
- [4] F. L. Lizzi, M. Astor, T. Liu, C. Deng, D. J. Coleman, and R. H. Silverman, "Ultrasonic spectrum analysis for tissue assays and therapy evaluation," *International Journal of Imaging Systems and Technology*, vol. 8, pp. 3-10, Sept. 1996.
- [5] F. L. Lizzi, M. Greenebaum, E. J. Feleppa, and M. Elbaum, Theoretical framework for spectrum analysis in ultrasonic tissue characterization, *Journal of the Acoustical Society of America*, vol. 73, pp. 1366-1373, April 1983.
- [6] M. F. Insana, R. F. Wagner, D. G. Brown, and T. J. Hall, Describing small-scale structure in random media using pulse-echo ultrasound, *Journal of the Acoustical Society of America*, vol. 87, pp. 179-192, Jan. 1990.
- [7] J. Mamou, M. L. Oelze, W. D. O'Brien, Jr., and J. F. Zachary, Identifying ultrasonic scattering sites from three-dimensional impedance maps, *Journal of the Acoustical Society of America*, vol. 117, pp. 413-423, Jan. 2005.
- [8] J. G. Proakis and D. G. Manolakis, *Digital Signal Processing*. Upper Saddle River, NJ: Pearson Prentice Hall, 2007.
- [9] M. F. Insana and T. J. Hall, Parametric ultrasound imaging from backscatter coefficient measurements: Image formation and interpretation, *Ultrasonic Imaging*, vol. 12, pp. 245-267, 1990.
- [10] P. Thevenaz and M. Unser, "A Pyramid Approach to Subpixel Registration Based on Intensity," *IEEE Transactions on Image Processing*, vol. 7, no. 1, pp. 27-41, 1998.